Egyptian Journal of Chemistry

http://ejchem.journals.ekb.eg/

Facile Route For The decoration of Nickel Hydroxide Sheets as Antibacterial Nanocomposite for Cellulose Acetate Butyrate Films

Emad S. Goda[1,2], M. A. Nour[2], Sang Eun Hong[1], Su bin lee[3], In Seop Kim[3], Kuk Ro Yoon[1], Heba Gamal[4*]

[1] *Organic Nanomaterials Lab, Department of Chemistry, Hannam University, Daejeon 305-811, Republic of Korea.*

[2] *Fire Protection Laboratory, National Institute of Standards, 136, Giza 12211, Egypt.*

[3] *Department of Biological Sciences and Biotechnology, Center for Biopharmaceuticals Safety Validation, Hannam University, Daejeon 305-811, Republic of Korea*

[4] *Home Economy Department, Faculty of Specific Education, Alexandria University, Alexandria, 21526, Egypt*

Abstract

The research for the development of antibiotic efficiency against bacteria responsible for common infections is considered of growing worldwide concern. Here, a facile and straight forward method for decorating nickel hydroxide sheets with polypyrrole-silver nanocomposite (Ppy-Ag) was developed by the interfacial polymerization of pyrrole monomer without using any reducing agent. The polypyrrole was used to facilitate the decoration and stabilization of AgNPs on the surface of nickel hydroxide sheets (NH). NH was synthesized using emulsion coprecipitation method. The thermal and morphological properties of the decorated NH have been investigated to confirm the existence of the polypyrrole wrapped layer. Cellulose acetate butyrate (CAB) films were also plasticized with polyvinyl pyrrolidone (PVP) in different mass ratios between PVP and CAB. The results showed that CAB film with 20 wt.% PVP gave the optimal values in terms of mechanical properties. The decorated NH were then added to CAB20 in various mass ratios (3, 6, 9 and 12%) achieving a very good compatibility and forming well dispersed nanocomposites films. The antibacterial activity, water permeability, contact angle and mechanical properties of the developed nanocomposite films were studied. The clear inhibition zone for the new nanocomposite films against S. aureus and E. coli bacteria was recorded as 25.33 ± 1 and 29 ± 1 mm, respectively. Furthermore, the water vapour permeability for the novel CAB nanocomposite films was found 68.83 g/m2/day achieving 29% reduction compared to the blank CAB20 (97.28g/m^2/day). Additionally, the mechanical properties were also significantly improved. The different materials were characterized using TGA, FTIR and SEM.

KEYWORDS: Nanocomposites; Nanostructures; dispersion; antibacterial activity; CAB films.

1. Introduction

Nowadays, a great attention is directed to the renewable and biodegradable materials because the products manufactured from petroleum-based polymers are single used materials and should be disposed continuously from the environment in order not to affect the health of surrounding living beings because they can release toxic by-products. Furthermore, there is a deplete in the fossil fuel used to produce these polymers besides the cost effect [1-3].

Cellulose derivatives are considered one of the most widely used biodegradable polymers. Further,

*Corresponding author e-mail: ardhan2007@yahoo.com
Receive Date: 23 June 2021, Revise Date: 21 July 2021, Accept Date: 25 July 2021
DOI: 10.21608/EJCHEM.2021.79268.4046

cellulose acetate butyrate (CAB) is found to be the most promising derivative of cellulose that can be used in many industrial applications instead of the non-biodegradable polymers from petroleum as it has approximately the same desired properties. However, CAB has high degree of brittleness that can restrict its applications [4,5]. The toughness of CAB could be improved using plasticizers such as PEG which are materials that have the ability to reduce the hydrogen bond interaction between the polymer chains [6]. Nickel hydroxide (NH) has garnered attention as a component of polymer composite because of its electrochemical properties [7]. It was previously reported that NH nanosheets had the advantages of better physicochemical properties and large specific surface area [8]. Nevertheless, NH has to be efficiently modified in order to achieve well dispersion in polymer obtaining polymer nanocomposite with improved mechanical properties. Meanwhile, most of the biodegradable polymers reveals no antibacterial activity which an issue guides the researchers and industrial field to be directed to the preparation of polymeric nanocomposites. Nanoparticles such as copper nanoparticles (CuNPs), AgNPs are commonly investigated as antibacterial nanomaterial for biopolymers [[9-12]. But, the AgNPs are susceptible to agglomerate results in the deterioration of the nanoparticles properties. In order to solve this problem, stabilizers should be used to decrease the surface energy of the particles and hence the aggregation of the AgNPs [13,14]. Various types of polymers have been utilised to stabilize the silver nanoparticles such as conducting polymers to find special applications like sensors and electronic devices [15,16]. It is pertinent to note that we have reported the functionalization of different nanomaterials using various methods [17-19]. Here, for the first time, a facile, novel and one-pot route for the decoration of nickel hydroxide sheets with polypyrrole silver nanocomposite was developed by an interfacial polymerization method. Ppy-Ag nanocomposite was expected to be successfully anchored on the surface of NH sheets. Then, nickel hydroxide-polypyrrole- silver nanocomposites (NH-PPy-Ag) were mixed with PVP plasticized CAB films to prepare novel antibacterial nanocomposites films. NH and NH-PPy-Ag were tested using FTIR, TGA and SEM to confirm the decoration process. The antibacterial activity, the water permeability, hydrophobicity and mechanical properties of the new nanocomposite films were also studied.

2. Experimental

2.1. Materials

Nickel chloride ($NiCl_2$, anhydrous), sodium dodecyl sulfate (SDS), ammonium hydroxide (NH_4OH), pyrrole, chloroform, silver nitrate and toluene were obtained from Sigma-Aldrich, USA, and were used for synthesis reactions as obtained without any further purification. Cellulose acetate butyrate (CAB), polyvinyl pyrrolidone (Average Mw =1300000) were obtained from Sigma-Aldrich, USA.

2.2. Synthesis of Nickel Hydroxide nanosheets (NH)

Nickel Hydroxide nanosheets was prepared based on our previous method [20]. In the synthesis, in a round bottom flask containing (100 mL) double distilled water, (2.97 g) nickel chloride and (0.29 g) SDS were dissolved and then magnetically stirred for 1 h. After that, 10 mL of 30 wt.% ammonia solution was added and followed by refluxing for 4h. Finally, the solution was left to cool at room temperature forming a green colour precipitate from nickel hydroxide. The precipitate was obtained by vacuum filtration and washing with distilled water. The product was dried at 70 °C until a constant weight.

2.3. Synthesis of NH-Ppy-Ag ternary nanocomposites

NH nanosheets have been decorated with silver nanoparticles using ultrasonication followed by oxidative interfacial polymerization of pyrrole. For synthesis, in a 25 ml beaker containing 0.575 g silver nitrate dissolved in 25 ml DIW, 50 mg of as-prepared NH was added, then the mixture was exposed to ultrasonication using ultrasonic with probe (model: sonosmasher) with the output power set at 50% for 30 min to produce a green homogenous dispersion which is considered the water phase. In another beaker, 0.125 ml of pyrrole was dissolved in 12.5 ml toluene to form the organic phase which was then added to the water phase dropwise. Finally, the mixture was exposed to magnetic stirring for 22 h. For making comparison, Ppy-Ag nanocomposite was also synthesized similar to the same method for NH-Ppy-Ag nanocomposite synthesis without the addition of NH.

2.4. Preparation of PVP plasticized CAB films

The CAB solutions were synthesized by dispersing a predetermined amount of CAB powder into 15 ml chloroform. After that, the plasticized CAB films were fabricated by dissolving of PVP in the CAB solution

with different mass ratios and then were stirred for 3 h at room temperature. The resultant solutions were then poured into a petri plate. The thin CAB films were obtained after the solvent was slowly evaporated at 50 °C. The sample compositions were shown in Table 1.

Table 1. The composition of CAB films.

Sample Name	CAB (wt%)	PVP (wt%)	NH-Ppy-Ag (wt%)	Ppy-Ag (wt%)
CAB	100	0	0	0
CAB_{10}	90	10	0	0
CAB_{20}	80	20	0	0
CAB_{30}	70	30	0	0
$CAB_{20}Ag_3$	80	20	3	3
$CAB_{20}N_3$	80	20	3	0
$CAB_{20}N_6$	80	20	6	0
$CAB_{20}N_9$	80	20	9	0
$CAB_{20}N_{12}$	80	20	12	0

2.4. Preparation of NH-Ppy-Ag/CAB nanocomposite films

The CAB nanocomposites were fabricated using solution blending method. The PVP (20 wt.%) was mixed into a previously prepared CAB solutions. A preweighted amounts of NH-PPy-Ag (3, 6, 9 and 12 wt%) were dispersed into 20 ml chloroform using sonication for 10min to form a homogenous suspension which was then added to the former PVP/CAB solutions with vigorous stirring for 3h to form CAB nanocomposites suspensions. Next, the resultant black dispersions were then poured into glass petri plate and placed in an oven at 50 °C for the slow evaporation of the solvent to form CAB nanocomposite films.

2.5. Characterization

Fourier transform infrared spectroscopy (FTIR) for NH and NH-Ppy-Ag was done using a FTIR spectrometer with the model: iS10, Nicolet Nexus, Minnesota. Meanwhile, the thermal analysis was conducted on SCINCO (TGA 1000) series thermal analyser with the conditions (heating rate (10 °C/min), from 25 to 600 °C, N_2 gas with flow rate 30 ml/min. Morphology studies were investigated using an emission scanning electron microscope (Mini-SEM SNE-4500M). A carbon disk was used to carry the sample using double-sided adhesive tape. The mechanical properties of the CAB films were determined using universal testing machine (Shimadzu/AG-500 KNG, Tokyo, Japan) where the films with a thickness 0.2 ± 0.05 mm were cut off into samples with length (20 ± 0.2 mm) and width (5 ± 0.2 mm). For the measurements, three samples were measured seperately.

For obtaining water vapor permeability (WVP) values, the standard BS 7209-1990 was used [21]. In detail, 46 mL DIW was added in a petri dish with diameter 80 mm at a temperature 20 ± 2 °C and was enveloped with different CAB films. After that, the initial mass of the dishes was obtained. After, the dishes were put on a turntable for 24 h, they were re-weighed to have the final mass. WVP is calculated in $g/m^2/day$ by using following equation:

$$WVP = \frac{24M}{At}$$

where M refers to the mass loss of the assembled dish in g, t is time in h and A is the film exposed area.

Water static contact angles of CAB nanocomposites were evaluated using SEO Phoenix 300 touch contact angle analyser. Antibacterial activity of the CAB films was investigated using agar well-diffusion method [22] against Gram-positive bacteria (S. aureus) and Gram-negative bacterium (E. coli) where, CAB nanocomposites films were silted into small discs with diameter (9 mm), and then were put into Mueller Hinton agar plates with bacteria of colony concentration 10^5–10^6 CFU/mL. Then, the plates were incubated at temperature 37 °C for 24 h. The bacterial growth inhibition zone diameter was used to determine the inhibition zones for the CAB films. For the statistical analysis, thee values were used.

Experimental data were statistically analyzed by analysis of variance (ANOVA) for three independent triplicates which were averaged and expressed as the mean ± standard error.

3. Results and discussion

3.1. Novel Synthesis of NH-Ppy-Ag Nancomposite

The decoration process of nickel hydroxide sheets with Ppy-Ag was easily developed by the interfacial polymerization of pyrrole monomer using silver nitrate as shown in scheme 1. The polypyrrole was used to facilitate

the deposition and stabilization of AgNPs on the surface of nickel hydroxide sheets (NH). Silver nitrate acts as an oxidizing agent for the pyrrole monomer. Nickel hydroxide in the form of nanosheets was firstly synthesized through emulsion coprecipitation method using sodium dodecyl sulfate (SDS) as an anionic surfactant and as a structure-directing agent based on our previous method [20]. For the preparation of NH-Ppy-Ag nancomposite, NH and $AgNO_3$ were dispersed in the aqueous phase and pyrrole was dissolved in toluene to form the organic phase for conducting the interfacial polymerization of polypyrrole. It was clearly found that Ppy-Ag nanocomposite was uniformly formed on the surface of NH nanosheets. The sulfate group from the NH preparation process and the oxygen-containing hydroxyl groups of NH acting as anchor sites, which can lead to the easily decoration of NH with AgNPs. Here, the interfacial polymerization method reveals a controllable and slow reaction compared to the conventional polymerization methods[23].

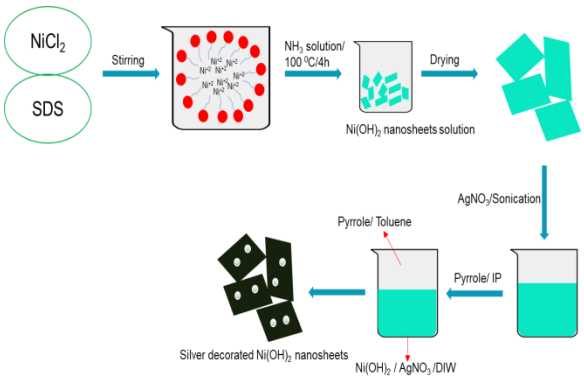

Scheme 1. Schematic synthesis of NH-PPy-Ag by interfacial polymerization method.

3.2. Characterization of developed NH-Ppy-Ag

The structures of NH, Ppy-Ag and NH-Ppy-Ag have been clearly investigated using IR spectroscopy. Fig. 1a shows the FTIR spectrum of the prepared pure NH where the sharp peak detected at 3647 cm^{-1} was attributed to the -OH groups stretching. Furthermore, the peaks seen at 2918 and 2852 cm^{-1} were assigned for the symmetrical and asymmetrical stretching absorption CH_2 of SDS, respectively. Moreover, the peak seen at 1062 cm^{-1} is for the symmetrical stretching absorption SO_2 due to the SO_3H functional group of the SDS [20].

Fig. 1b shows the characteristic absorption peaks of Ppy-Ag. The vibrations found at 1544 and 1465 cm^{-1} represented the symmetric and antisymmetric pyrrole ring. The absorption peaks at 1307 and 1202 cm^{-1} related to in plane = CH and C-N stretching bands representing the oxidized and doped PPy, respectively. The sharp absorption peak observed at 1385 cm^{-1} corresponds to the presence of nitrate ion as dopant or counter ion helps in charge neutralization of the polymer backbone [24]. Furthermore, the peak sited at 3457 cm^{-1} may be attributed to NH stretching of the Ppy [25]. The characteristic peaks presented at 780 and 933 cm^{-1} might be for the C-H and C-C out of plane deformations. On the other hand, all characteristic peaks for Ppy-Ag nanocomposite and pure NH were clearly found in the same positions in NH-Ppy-Ag nanocomposite (Fig. 1c). Interestingly, there is a slight shift in the peaks observed at 1183, 932 and 796 cm^{-1} in case of NH-Ppy-Ag nanocomposite compared to the Ppy-Ag nanocomposite peaks. This might be indicating the strong supramolecular interactions between the NH and Ppy-Ag nanocomposite, leading to the successful synthesis of NH-Ppy-Ag nanocomposite.

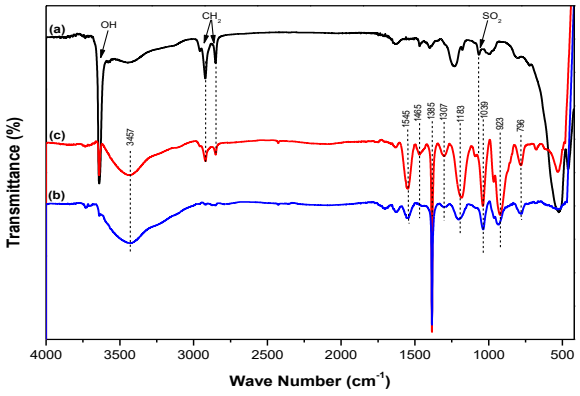

Fig. 1. FTIR spectra of NH (a), NH-Ppy-Ag (b) and Ppy-Ag (c).

Furthermore, the TGA curve for Ppy-Ag was found in Fig. 2b where the thermal analysis involves two steps, the first step was below 200 °C related to the evolution water vapour adsorbed on the polymer surface and the second peak involves weight loss between 200 and 560 °C corresponds to the thermal breaking of Ppy leaving a char yield of 66.4% [26]. On the other hand, NH-Ppy-Ag nanocomposite shows three decomposition peaks (Fig. 2c). The first step with mass loss 4% is from the moisture loss. The

second peak observed in the range 260 and 390 °C with weight loss~7% due to the decomposition of SDS and the hydroxyl group of NH [20]. The decomposition of Ppy was shown on the third peak with temperature range from 400°C and to 570 °C with sharp mass loss (~19%) revealing the formation of NH-Ppy-Ag nanocomposite. Furthermore, from the TGA results, NH-Ppy-Ag nanocomposite had higher char yield (70%) compared to Ppy-Ag nanocomposite (66.7%) showed better thermal stability from the existence of nickel hydroxide nanosheets in the nanocomposite.

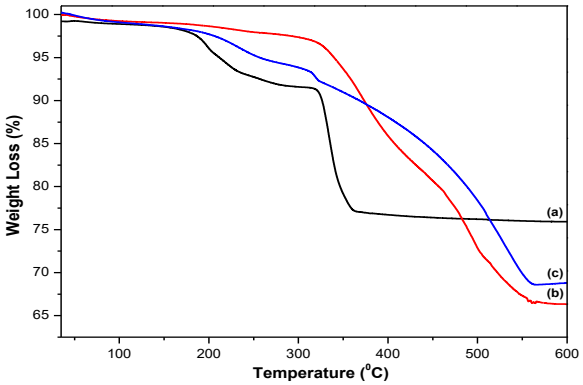

Fig. 2. TGA curve of NH (a), Ppy-Ag (b) and NH-Ppy-Ag (c).

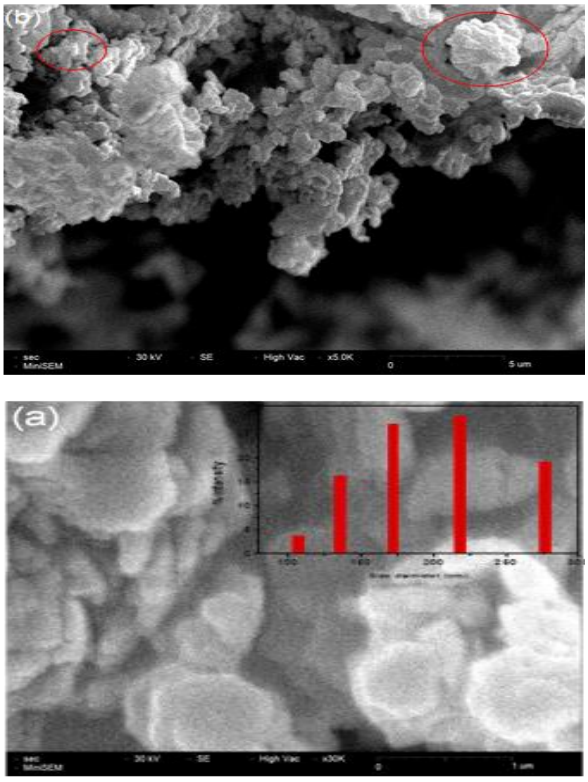

Fig. 3. SEM images of NH (a) and NH-Ppy-Ag (b).

The surface morphology of $Ni(OH)_2$ and NH-Ppy-Ag was investigated using SEM as depicted in Fig. 3. where NH reveals a well uniform nanosheet loosely packed structure (Fig. 3a) in diameter approximately 300 nm in agreement with our previous report [20]. Also, to measure the size of NH sheets, DLS experiment is conducted and was found as inset in Fig. 3. where the range of particles size from 106–277 nm as it was also found from SEM analysis. On the other hand, Fig. 3b shows SEM image of NH-PPy-Ag nanocomposite displayed the growth and wrapping of polypyrrole nanoparticles on the surface of NH giving nanocomposite with irregular shape and an increase in the overall diameter of NH sheets after the functionalization process of their surface. This confirms the successful modification of NH sheets with polypyrrole polymer and hence the decoration with AgNPs emphasizing the synthesis of NH-Ppy-Ag nanocomposite.

3.2. Characterization of CAB nanocomposites films

The nanocomposites films of CAB with different NH-Ppy-Ag were synthesized using solution mixing method in chloroform as a solvent. SEM technique was used to check the surface morphology of the CAB nanocomposite film. Fig. 4a shows the surface scanning of pure CAB_{20} which is very smooth. Meanwhile, Fig. 4b reveals the dispersion of NH-Ppy-Ag in CAB which are well uniformly dispersed in CAB polymer forming CAB-NH-Ppy-Ag nanocomposite as pointed by arrows. It can be found that the hydrogen bonding interaction between NH-Ppy-Ag and the polymer is the main cause for the good compatibility and well dispersion resulting in a stronger interfacial adhesion.

Thermal behaviour for CAB films were investigated using TGA and surfaced in Fig. 5. The TGA curve of pure CAB film was manifested in Fig. 5a which shows one decomposition step with a temperature range 275–410 °C leaving chare yield ≈ 2.5% attributing to the breaking of CAB polymer chains [27]. It can be also found that the addition of PVP in CAB with 20 wt.% improves the thermal stability of CAB (Fig. 5b) as it delays the temperature required for 50% weight loss from 358 to 370 °C with much more char yield (9.34%). This is due to the strong interactions as a result of the formed hydrogen bonding between CAB and PVP molecules. On the other hand, when mixing NH-Ppy-Ag nanosheets to CAB polymer in different mass ratios, the temperature for 50% weight loss increases from 358°C to 360,

362.5, 367 and 370°C with the mass loading 3,6,9,12% respectively, compared to the virgin CAB. Interestingly, the char yield also increases from 2.5 to 14 % with increasing the mass loading ($CAB_{20}N_{12}$). This is might be due to the well dispersion of NH-Ppy-Ag in CAB helps in enhancing the charring tendency for the polymer. Moreover, prior research has thoroughly investigated that poly pyrrole chain containing nitrogen species can act as an efficient char forming agent resulting in forming a strong char barrier protects polymer nanocomposites from excessive decomposition [28].

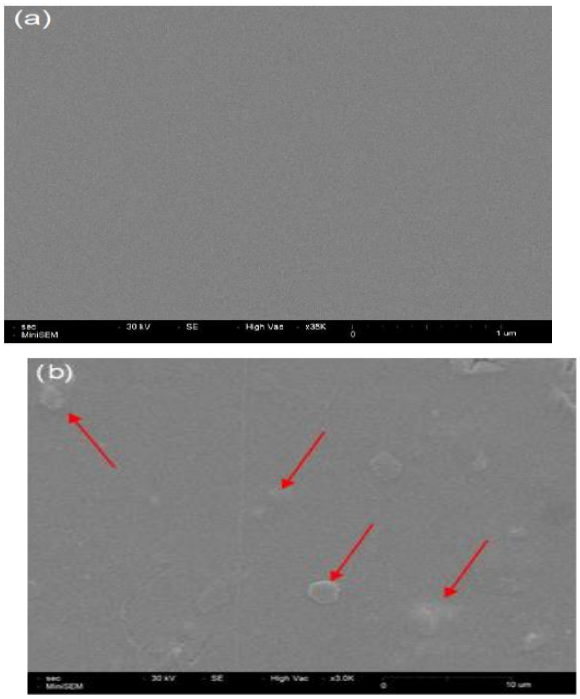

Fig. 4. SEM images of blank CAB_{20} (a) and $CAB_{20}N_3$ nanocomposite film (b).

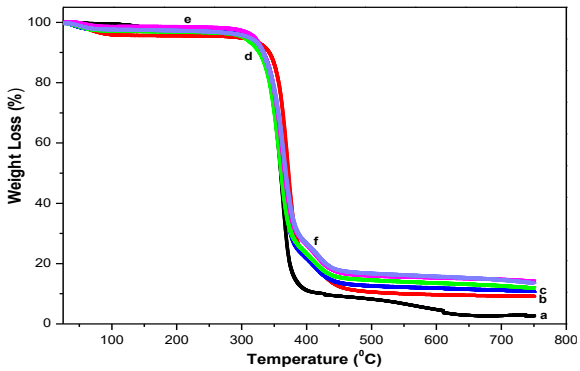

Fig.5. TGA curve of CAB (a), CAB_{20} (b), $CAB_{20}N_3$ (c), $CAB_{20}N_6$ (d), $CAB_{20}N_9$ (e) and $CAB_{20}N_{12}$ (f).

Plasticizer is a material that has the ability to decrease the polymer brittleness by improving the elongation at break [29]. The pure CAB is found to be brittle in nature [6]. In this study, PVP acts as a plasticizer for obtaining flexible CAB films. Table 2 provides the mechanical properties of CAB films mixed with PVP polymer in different mass ratios. As can be seen from the table, the tensile strength is found to be in inversely proportion with the elongation. Moreover, when increasing the plasticizer mass ratios in CAB films up to 20 wt.%, the elongation at break (%) is significantly increases from 10.12 to 64.75% and the tensile strength decreases from 30 to 27.45 MPa in a relation with the pure CAB. However, in case of 30 wt.% mass ratios, the rate of increase is less. It was stated that the plasticizer with 20wt.% can reach its maximum effect into CAB films [6]. On the other hand, the rate of decrease for the tensile strength is remarkedly beyond 20 wt% loading of PVP. Consequently, CAB_{20} was chosen for the fabrication of CAB nanocomposites films filled with NH-PPy-Ag in different mass ratios.

Additionally, the overall essential aim of adding a small amount of decorated NH sheets into CAB polymer is to improve its mechanical properties. This enhancement in mechanical properties may be because of the stronger interfacial interaction between NH-Ppy-Ag and the matrix CAB, which comes from two factors, the hydrogen bonds found between the polypyrrole wrapped nickel hydroxide sheets and CAB in addition the better dispersion of these nanosheets in the polymer matrix. In order to prove this hypothesis, we studied the typical stress−strain curves, tensile strength and elongation at break for CAB and NH-PPy-Ag/CAB nanocomposite which are depicted in Fig. 6,7.

Table 2. Mechanical properties of CAB Films and their nanocomposites.

Sample Code	CAB/PVP	Tensile strength (MPa)	Elongation at break (%)
CAB	100:0	30.00 ± 1.20	10.12 ± 0.90
CAB_{10}	90:10	28.70 ± 4.95	16.78 ± 3.14
CAB_{20}	80:20	27.45 ± 3.39	64.75 ± 2.62
CAB_{30}	70:30	27.00 ± 0.59	68.50 ± 4.50

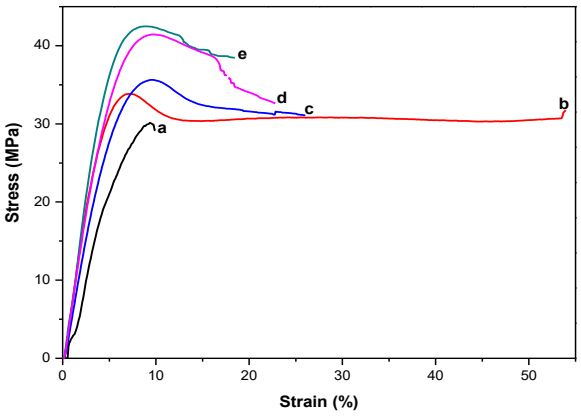

Fig. 6. Stress–strain curve of CAB (a), $CAB_{20}N_3$ (b), $CAB_{20}N_6$ (c), $CAB_{20}N_9$ (d) and $CAB_{20}N_{12}$ (e).

It can be obviously derived from the stress vs strain curve shown in Fig. 6, the tensile strength and % elongation at break, respectively (Fig. 7). It can be apparently seen from Fig. 7a that when decorated NH sheets were incorporated into CAB with mass loading 3, 6, 9 and 12% results in a significant increase of the tensile strength of CAB from 30 to 31.8, 35.6, 41.4 and 42.5 consecutively achieving an increase 41% for $CAB_{20}N_{12}$ nanocomposite film compared to the pure CAB. This may be related to the increase of the extent of hydrogen bonding between NH-Ppy-Ag and CAB, as mentioned earlier. Consequently, NH-Ppy-Ag has a reinforcing effect when incorporating in the nanocomposites. This fact was previously stated for various nanocomposites prepared from different polymers and polymer blends [30-32].

In the same time, the elongation at break (%) of the virgin CAB increases when mixed with PVP as plasticizer and decorated NH. However, for the CAB nanocomposites, it decreases from 53.39 to 26.1, 22.8 and 18.46 % with increasing the mass loading of NH-PPy-Ag filler from 3% to 6, 9 and 12% respectively (Fig.7) which is due to the reinforcing action of NH-Ppy-Ag in CAB films causing the restriction of the polymer chains mobility.

It is necessary to study the effect of NH-PPy-Ag on the water vapour permeability (WVP) of CAB films. WVP measures and adjusts the flow of water molecules through films to the surrounding environment. Thus, WVP has to be diminished as possible to protect the products from the dehydration [33]. WVP for CAB nanocomosites films were tested and the results are revealed in Table 4. As it can be found from Table 4, the WVP of CAB_{20} was 97 g/m^2/day which decreases to 85.58, 83.85, 74.33 and 68.83 g/m^2/day, respectively with the addition of the mass ratios 3, 6, 9, 12% of NH-PPy-Ag into CAB_{20} film achieving maximum decrease of 30%. Thus, the existence of decorated NH into the polymer matrix can form a sinuous way that decreases the passage of water vapor across the film.

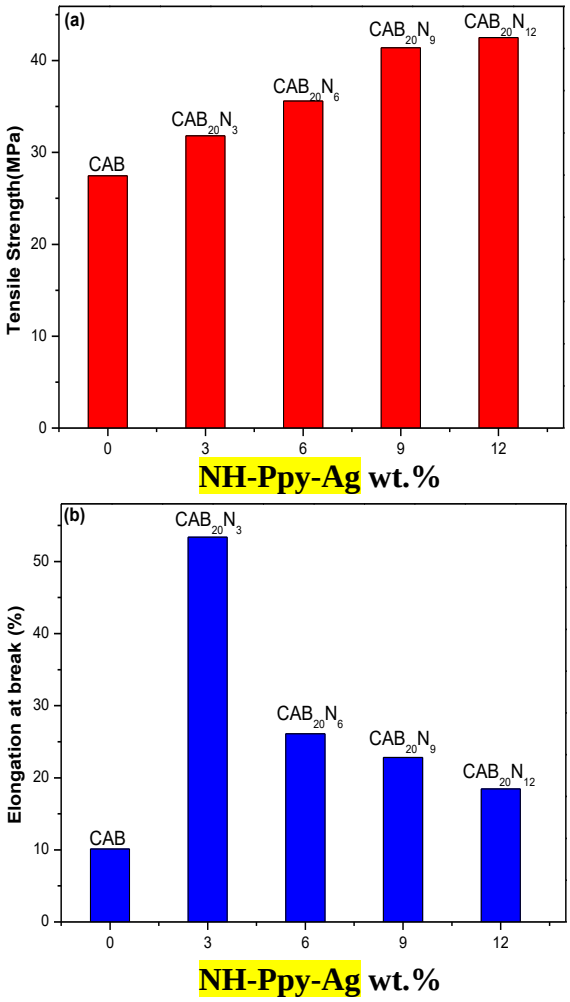

Fig.7. Tensile strength (a), and elongation at break (b) of pure CAB and their different nanocomposites.

Table 3. Water vapor permeability of CAB films and their nanocomposites.

Sample Code	Water Vapor Permeability (WVP) [g/m^2/day]
CAB_{20}	97.28
$CAB_{20}N_3$	85.58
$CAB_{20}N_6$	83.85
$CAB_{20}N_9$	74.33
$CAB_{20}N_{12}$	68.83

The surface energy of CAB films was evaluated using the values of contact angle measurements which gives information about essential properties like wettability and adhesion. This method can be used to estimate the interfacial and surface free energy. Furthermore, the wetting parameter can find a great interest in different industrial applications, such as coating, lubrication, oil recovery, and printing [34]. For this test, a sessile drop method was performed where contact angle was calculated from the angle tangent between the substrate surface and one water droplet at room temperature. From the results in Table 4, it can be noticed that the hydrophilicity of CAB films decreased with the addition of different mass loading of NH-Ppy-Ag. The blend between CAB and PVP manifests high hydrophilicity and reactivity with water because of existence of hydroxyl groups and carbonyl groups in their structure and can interact with water via hydrogen bonding results in an increase in the hydrophilicity and the solubility in water. Meanwhile, in case of using NH-Ppy-Ag as fillers for CAB film, the hydrogen bonding was found between the hydroxyl groups of CAB/PVP film and the functional groups of NH-Ppy-Ag lowering the chance of occurring hydrogen bonding between the polymer and water molecules. Consequently, the hydrophilicity of CAB film decreased with increasing the mass ratios of NH-Ppy-Ag [35].

Two bacteria strains comprising E. coli and S. aureus have been chosen for conducting antibacterial tests because they are usually the main reason for all the medical-associated infections [34]. The antibacterial activity of different CAB nanocomposites against E. coli and S. aureus was investigated using the disc diffusion method as shown in Fig. 8 and the diameters of zone of inhibition were measured as depicted in Table 5.

Table 4. Contact angle values of CAB films and their different nanocomposites

Sample Code	Contact angle (θ)
CAB_{20}	41.8
$CAB_{20}N_3$	57.6
$CAB_{20}N_6$	72.4
$CAB_{20}N_9$	75.8
$CAB_{20}N_{12}$	75.6

Table 5. Antibacterial properties of the CAB films using agar well-diffusion method.

Sample Code	S. aureus	E. coli
	Inhibition Zone (mm)	
CAB_{20}	0	0
$CAB_{20}Ag_3$	0	0
$CAB_{20}N_3$	13.3 ± 0.57	17.3 ± 0.57
$CAB_{20}N_6$	18.3 ± 0.57	20.0 ± 1.0
$CAB_{20}N_9$	22.3 ± 1.0	25.3 ± 0.57
$CAB_{20}N_{12}$	25.3 ± 1.0	29.0 ± 1.0

It can be clearly observed from the result, that CAB_{20} film does not have an antimicrobial activity against two strains. Nevertheless, the CAB nanocomposites films with various NH-Ag-Ppy mass ratios considerably diminish the growth of two types of bacteria in nutrient agar plates (Fig. 8). Moreover, it is obviously seen that with commingling the mass ratios of 3, 6, 9 and 12 wt.% of NH-PPy-Ag with CAB_{20} polymer, the zone inhibitions are recorded 13.3, 18.3, 22.3 and 25.3 mm against S. aureus and 17.3, 20.0, 25.3 and 29.0 mm against E. coli, respectively revealing the remarkable increase of the inhibition zone and the strong effect against the bacteria growth. Interestingly, when adding mass ratio 3wt.% of Ag-Ppy in CAB_{20} gives nanocomposite which shows no effect against the bacteria growth, even the nanocomposite contains silver nanoparticles. These results show the successive decoration process of nickel hydroxide sheets with silver nanoparticles and its significant impact on the bacteria growth. It is also pertinent to note that E. coli reveals a larger zone of inhibition compared to S. aureus. The variance in the inhibition zone diameter may be attributed to the susceptibility of bacteria against to the prepared CAB/NH-Ppy-Ag nanocomposite films. Therefore, it can be concluded from the present study that NH-Ppy-Ag nanocomposite show an efficient antibacterial activity against both Gram negative and positive bacteria and can be used in biomedical applications. It is noteworthy to note that our NH-Ppy-Ag/ CAB nanocomposite can be used as sensors for the detection of analytes due to the excellent electric properties of nickel hydroxide and poly pyrrole [36].

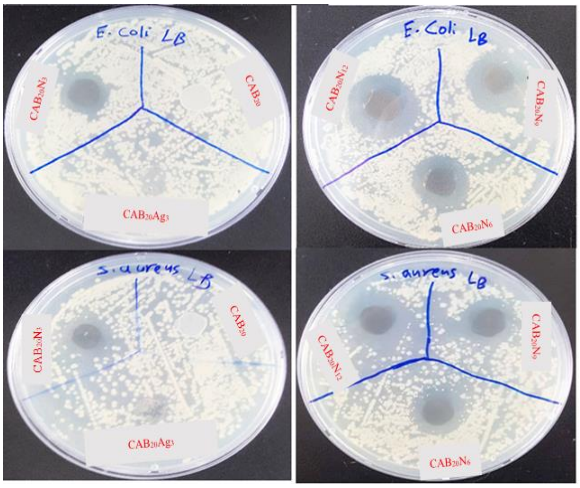

Fig. 8. Photograph of antimicrobial test results of CAB_{20}, $CAB_{20}Ag_3$ and their different nanocomposite films against S.aureus and E.coli.

4. Conclusion

A facile and one pot method for the decoration of NH and forming the NH-PPy-Ag ternary nanocomposite has been successfully developed. The PPy-Ag was clearly deposited on NH sheets. The existence of pyrrole plays a vital role in the decoration process as its polymerization help in the formation of AgNPs on the surface of NH sheets. CAB films were successfully plasticized with PVP revealing that 20wt.% PVP has the best mechanical properties. NH-PPy-Ag were then used as fillers with CAB films in different mass ratios achieving a very good compatibility and forming well dispersed nanocomposites films. The antibacterial activity, the water permeability and mechanical properties of the new nanocomposites films were investigated. The clear inhibition zone for the new developed nanocomposite films against staphylococcus aureus bacteria and Escherichia coli was recorded as 25.33 ± 1 and 29 ± 1mm ($CAB_{20}N_{12}$ Nanocomposite), respectively. Furthermore, the water vapour permeability for the novel CAB nanocomposite films was found 68.83g/m^2/day achieving reduction 29% compared to the blank CAB_{20} (97.28g/m^2/day). The mechanical properties were also markedly improved as the tensile strength shows an increase 41% for $CAB_{20}N_{12}$ nanocomposite film compared to the pure CAB. It can be concluded also from contact angle measurements that NH-PPy-Ag decreases the hydrophilicity of CAB film by lowering the hydrogen bonding with water molecules.

References

[1] .A. Gross, B. Kalra, Biodegradable Polymers for the Environment, Sci. 297 (2002) 803−807.
[2] L. Avérous, Biodegradable Multiphase Systems based on Plasticized Starch: A Review, J. Macromol. Sci. Polym. Rev. 44 (2004) 231−274.
[3] A. Södergård, M. Stolt, Properties of Lactic Acid based Polymers and their Correlation with Composition, Prog. Polym. Sci. 27 (2002) 1123−1163.
[4] D. Wang, G. Sun, Formation and morphology of cellulose acetate butyrate (CAB)/polyolefin and CAB/polyester in situ microfibrillar and lamellar hybrid blends, Eur. Polym. J. 43 (2007) 3587–3596.
[5] D. Wang, G. Sun, B.S. Chiou, A high throughput, controllable and environmentally benign fabrication process of thermoplastic nano-fibers, Macromol. Mater. Eng. 292 (2007) 407-414.
[6] N.R. Saha, I. Roy, G. Sarkar, A. Bhattacharyya, R. Das, D. Rana, R. Banerjee, A.K. Paul, R. Mishra, D. Chattopadhyay, Development of active packaging material based on cellulose acetate butyrate/polyethylene glycol/aryl ammonium cation modified clay, Carbohydr. Polym. 187 (2018) 8–18.
[7] Y. Xing, G. Gao, G. Zhu, J. Gao, Z. Ge, H. Yang, A Nonenzymatic Electrochemical Glucose Sensor Based on $Ni(OH)_2$-CNT-PVDF Composite and Its Application in Measuring Serum Glucose, J. Electrochem. Soc. 161 (2014) B106-B110.
[8] W. Lana,Y. Suna, Y. Chen, J. Wang, G. Tang, W. Dou, Q. Su, E. Xie, Ultralight and Flexible Supercapacitor Electrodes Made from the $Ni(OH)_2$ Nanosheets doped with Ag Nanoparticles/3D Graphene Composite, RSC Adv. 5 (2015) 20878-20883.
[9] J. George, V.A. Sajeevkumar, K.V. Ramana, S.N. Sabapathy, Siddaramaiah. Augmented Properties of PVA Hybrid Nanocomposites Containing Cellulose Nanocrystals and Silver Nanoparticles, J. Mater. Chem. 22 (2012) 22433−22439.
[10] S.K. Sehmi, S. Noimark, J. Weiner, E. Allan, A.J. MacRobert, I.P. Parkin, Potent Antibacterial Activity of Copper Embedded into Silicone and Polyurethane, ACS Appl. Mater. Interfaces. 7 (2015), 22807−22813.
[11] T.T. Nguyen, O.H. Chung, J. S. Park, Coaxial Electrospun Poly(lactic acid)/Chitosan (Core/Shell) Composite Nanofibers and their Antibacterial Activity, Carbohydr. Polym. 86 (2011) 1799−1806.
[12] N. Vigneshwaran, R.P. Nachane, R.H. Balasubramanya, P.V. Varadarajan, A Novel One-pot Green Synthesis of Stable Silver Nanoparticles Using Soluble Starch, Carbohydr. Res. 341 (2006) 2012−2018.
[13] P. Raveendran, J. Fu, S.L. Wallen, A Simple and "Green" Method for the Synthesis of Au, Ag and Au-Ag Alloy Nanoparticles, Green Chem. 8 (2006) 34−38.
[14] X. Xu, Y.Q. Yang, Y.Y. Xing, J.F. Yang, S.F. Wang, Properties of Novel Polyvinyl Alcohol/cellulose Nanocrystals/Silver Nanoparticles Blend Membranes, Carbohydr. Polym. 98 (2013) 1573−1577.
[15] K.H. Kate, S.R. Damkale, P.K. Khanna, G.H. Jain, Nano-silver mediated polymerization of pyrrole: Synthesis and gas sensing properties of polypyrrole

(PPy)/Ag nano-composite, J. Nanosci. Nanotechnol. 11 (2011) 7863-7869.
[16] Y.C. Liu, Sandwiched structure of Ag/polypyrrole/Au to improve the surfaced-enhanced Raman scattering, Electrochem. commun. 7 (2005) 1071-1076.
[17] J.H. Yang, B. Ramaraj, K.R. Yoon, Preparation and characterization of superparamagnetic graphene oxide nanohybrids anchored with Fe_3O_4 nanoparticles, J. Alloys. Compd. 583 (2014) 128–133.
[18] S.Y. Kim, B. Ramaraj, K.R. Yoon, Preparation and characterization of polyvinyl alcohol-grafted Fe3O4 magnetic nanoparticles through glutaraldehyde, Surf. Interface Anal. 44 (2012) 1238–1242.
[19] J. Ryu, B. Ramaraj, K.R. Yoon, Surface functionalization of multi-walled carbon nanotubes through surface-initiated atom transfer radical polymerization of glycidyl methacrylate, Surf. Interface Anal. 41 (2009), 303–309.
[20] B.S. Singu, U. Male, S.E. Hong, K.R. Yoon, Synthesis and performance of nickel hydroxide nanodiscs for redox supercapacitors, Ionics (Kiel). 22 (2016) 1485-1491.
[21] BS 7209:1990, Specification for water vapour permeable apparel fabrics, British Standards Institution, London, UK, (1990).
[22] R. Miles, S. Amyes, Laboratory control of antimicrobial therapy, Mackie and McCartney Practical Medical Microbiology, 14 (1996) 151-178.
[23] C. Bora, S.K. Dolui, Fabrication of polypyrrole/graphene oxide nanocomposites by liquid/liquid interfacial polymerization and evaluation of their optical, electrical and electrochemical properties, Polym. 53 (2012) 923-932.
[24] B. Singu, K.R. Yoon, Mesoporous polypyrrole-Ag nanocomposites for supercapacitors, J. Alloys Compd. 742 (2018) 610-618.
[25] A. Singh, Z. Salmi, N. Joshi, P. Jha, P. Decorse, H. Lecoq, S. Lau-Truong, M. Jouini, D.K. Aswal, M.M. Chehimi, Electrochemical investigation of free-standing polypyrrole–silver nanocomposite films: a substrate free electrode material for supercapacitors, RSC Adv. 3 (2013) 24567- 24575.
[26] P.K. Kalambate, R.A. Dar, S.P. Karna, A.K. Srivastava, High performance supercapacitor based on graphene-silver nanoparticles-polypyrrole nanocomposite coated on glassy carbon electrode, J. Power Sources. 276 (2015) 262-270.
[27] D. Mondal, M.M.R. Mollick, B. Bhowmick, D. Maity, M.K. Baina, D. Rana, et al, Effect of poly(vinyl pyrrolidone) on the morphology and physical properties of poly(vinyl alcohol)/sodium montmorillonite nanocomposite films. Prog. Nat. Sci-Mater. 23 (2013) 579–587.
[28] N. F. Attia, Organic nanoparticles as promising flame retardant materials for thermoplastic polymers, J. Therm. Anal. Calorim. 127 (2017) 2273–2282.
[29] T.H. McHugh, J.M. Krochta, Sorbitol- vs glycerol-plasticized whey protein edible films: Integrated oxygen permeability and tensile property evaluation. J. Agric. Food. Chem. 42 (1994) 841–845.
[30] D. Mondal, B. Bhowmick, M.M.R. Mollick, D. Maity, A. Mukhopadhyay, D. Rana, et al. Effect of clay concentration on morphology and properties of hydroxypropyl methyl cellulose films, Carbohydr. Polym. 96 (2013) 57–63.
[31] J. Rhim, Effect of clay contents on mechanical and water vapor barrier properties of agar-based nanocomposite films, Carbohydr. Polym. 86 (2011) 691–699.
[32] N.R. Saha, G. Sarkar, I. Roy, D. Rana, A. Bhattacharyya, A. Adhikari, et al. Studies on methylcellulose/pectin/montmorillonite nanocomposite films and their application possibilities. Carbohydr. Polym. 136 (2016) 1218–1227.
[33] N. Gontard, S. Guilbert, J.L. CUQ, Edible wheat gluten films: influence of the main process variables on film properties using response surface methodology, J. Food. Sci. 57 (1992) 190-195.
[34] S.P. Thoma, S. Thomas, R. Abraham, S. Bandyopadhyay, Polystyrene/calcium phosphate nanocomposites: contact angle studies based on water and methylene iodide, Express Polym. Lett. 2 (2008) 528-538.
[35] S. Mallakpour, M. Khani, Thermal and morphological studies of poly(vinyl alcohol)/poly(vinyl pyrrolidone)/ organoclay nanocomposites containing L-leucine moiety Colloid Polym. Sci. 294 (2016) 583-590.
[35] A.F. de Faria, D.S.T. Martinez, S.M.M. Meira, A.C.M. de Moraes, A. Brandelli, A.G.S Filho, O.L. Alves, Anti-Adhesion and Antibacterial Activity of Silver Nanoparticles Supported on Graphene Oxide Sheets, Colloids Surf. B 113 (2014) 115−124.
[36] D. Rao, Q. Sheng, J. Zheng, Novel Nanocomposite of Chitosan-protected Platinum Nanoparticles Immobilized on Nickel Hydroxide: Facile Synthesis and Application as Glucose Electrochemical Sensor, J. Chem. Sci. 128 (2016) 1367–1375.